JOURNAL OF MATERIALS SCIENCE 24 (1989) 2076–2080

Formation of stable and metastable phases in Al–Mn alloys by the use of a gravity chill casting technique

J. A. JUAREZ-ISLAS, D. H. WARRINGTON, H. JONES
Division of Metals, School of Materials, University of Sheffield, Sheffield S1 3JD, UK

The structures present in taper-section chill casting of hypereutectic Al–Mn alloys containing between 5 and 18 wt% Mn have been studied by optical metallography, X-ray diffractometry and microanalysis, in order to relate intermetallic phases such as the Al_6Mn and Al_4Mn obtained at low freezing rates with metastable structures such as the decagonal and icosahedral phase obtained at high cooling rates.

1. Introduction

Considerable interest has been evident in the study of quasi-crystalline phases, since the remarkable discovery by Shechtman *et al.* [1] of a phase in the rapidly solidified Al–14 wt % Mn alloy exhibiting an electron diffraction pattern which has sharp spots, but with five-fold symmetry axes which are not consistent with crystal lattice translations. This finding has stimulated a considerable amount of work on the formation of different metastable phases by rapid solidification of Al–Mn alloys [2–6], using techniques such as melt spinning [2], electron beam surface melting [5] and cooling of emulsions of fine droplets [6].

The approach of the work presented here, by use of a very simple casting technique, was to obtain a range of cooling rates during solidification by casting several Al–Mn alloys into a wedge-section copper mould, so that the range of micromorphologies linking the slowly and rapidly cooled might be obtained within a single ingot for each alloy composition.

2. Experimental procedure

Al–Mn alloys containing 5, 10, 15 and 18 wt % Mn were made by induction melting of high purity (99.99 wt %) aluminium and electrolytic (99.70 wt %) manganese in alumina crucibles.

The alloys were cast at 200 K superheat above the liquidus temperature into a wedge-shaped copper mould of dimensions shown in Fig. 1. Thermocouples were introduced through the side of the mould and were located centrally at 20, 55 and 80 mm from the top of the mould cavity, at which the cavity half-thickness was 9, 5 and 1.5 mm, respectively. Thermocouple outputs were recorded on a Goerz model 460 ElectroServoscribe chart recorder indicating cooling rates for Al–Mn alloys of ~ 21, ~ 47 and $\sim 150\,K\,sec^{-1}$, for the upper, middle and lower thermocouple positions, respectively.

Ingots were sectioned longitudinally and centrally in the plane normal to the diverging wedge faces, and then mechanically polished and etched in Murakami's reagent (10 g $K_3Fe(CN)_6$, 10 g NaOH and 100 ml H_2O), in order to reveal the different intermetallic phases present in each ingot section. The regions of characteristic morphology were located by optical microscopy. Samples of certain regions were removed for X-ray diffraction with filtered Cu$K\alpha$ radiation. Corresponding manganese contents of the extended α-alumina solid solution and intermetallic phases were determined by electron microscope microanalysis using a spot size of 64 nm and 30° of tilt in a Philips PSEM 500 electron microscope at 25 kV with reference to pure aluminium and manganese as standards.

3. Results and discussion

The locations of characteristic structure zones obtained in the ingots of the four Al–Mn alloys can be summarized in Fig. 2. The same figure indicates the locations a, b and c (shown by circles) where thermocouples were positioned in order to determine the

TABLE I Results of SEM microanalysis of intermetallics in wedge chill-cast Al–Mn alloys

Experimental conditions		Resulting intermetallic phase			
Alloy composition (wt %)	Cooling rate ($K\,sec^{-1}$)	Composition			Identity
		Al (at %)	Mn (at %)	Al:Mn	
Al–5 Mn	21	85.7	14.3	6.0	Al_6Mn
Al–10 and 15 Mn	21	81.5	18.5	4.4	Al_4Mn
Al–18 Mn	47	73.3	26.7	2.7	$Al_{11}Mn_4$
Al–10 and 15 Mn	47	85.2	14.1	6.0	Decagonal
Al–15 Mn	150	79.7	20.3	3.9	Icosahedral

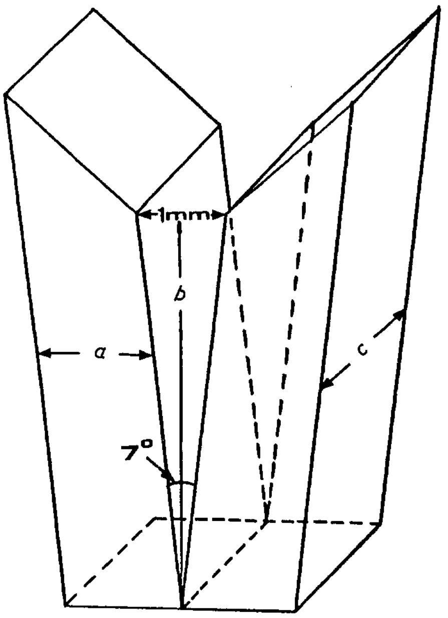

Figure 1 The mould used for gravity chill-casting technique. Dimensions of mould; *a* thickness = 25 mm, *b* length = 102 mm, *c* width = 38 mm.

freezing conditions achieved in the experiment. The measured cooling rates over the temperature range 950 to 750° C for the representative Al–10 wt % Mn alloy varied from approximately 21 K sec^{-1} (measured at position a) to approximately 47 K sec^{-1} (measured at position b) and approximately 150 K sec^{-1} (measured at position c). Figure 3 shows typical cooling curves from which the cooling rates at the three positions in the ingot were obtained.

The structure zones identified in Fig. 2, in terms of their primary phase, were of six main types as identified by microanalysis and/or X-ray diffractometry.

1. Primary α-Al solid solution plus interdendritic eutectic in ingots of Al–5 and 10 wt % Mn (Fig. 4a). The manganese contents of the α-Al solid solutions determined by SEM microanalysis in those ingots were 4.02 ± 0.42 and 4.63 ± 0.34 wt %, respectively, which once again confirm the ready susceptibility of Al–Mn alloys to form extended solid solutions (e.g. [7]).

2. Al_6Mn plus cellular α-Al solid solution was observed in ingots of Al–5, 10 and 15 wt % Mn. Although the normal crystal habit of primary Al_6Mn is diamond-shaped, most often incomplete or hollow [8], as was observed in Al–5 wt % Mn, its morphology was dendritic in ingots of Al–10 and 15 wt % Mn (Fig. 4b). Identification of this intermetallic was carried out by means of X-ray diffractometry (Fig. 5a) and SEM microanalysis (see Table I), which confirmed the equilibrium stoichiometry Al_6Mn.

3. Al_4Mn plus cellular α-Al solid solution, frequently showing a crystal habit of well-formed hexagonal needles [9], as is how in Fig. 4c, was observed in ingots of Al–10 and 15 wt % Mn. Figure 5b shows the X-ray diffraction pattern obtained from specimens containing this intermetallic, which shows also the presence of Al_6Mn possibly as interdendritic eutectic (Fig. 4c). Once again, the equilibrium stoichiometry (Al_4Mn, Table I) was confirmed by SEM microanalysis.

4. LT-$Al_{11}Mn_4$ plus α-Al solid solution was observed in an ingot of Al–18 wt % Mn, as a fine bundle of platelets, as is shown in Fig. 4d. SEM microanalysis carried out in those platelets, showed a composition of 57.4 wt % Al (73.3 at %) and 42.6 wt % Mn (26.7 at %). Figure 5c shows the X-ray diffraction pattern of the microstructure containing this intermetallic.

5. Decagonal (otherwise known as T-) phase in α-Al solid solution was observed in ingots of Al–10 and 15 wt % Mn. In the Al–10 wt % Mn, the decagonal phase was observed as nodules which showed a central nucleus, from which dendrites grew radially due to morphological and crystallographic effects, and stopped at the grain boundary, as is shown in Fig. 4e. In the Al–15 wt % Mn alloy, the decagonal phase was observed as randomly oriented crystals, as part of a large dendritic system, as is shown in Fig. 4f. Figure 5d shows typical X-ray diffraction intensity peaks (in the range $38 < 2\theta < 46°$ with Cu$K\alpha$ radiation), for this phase.

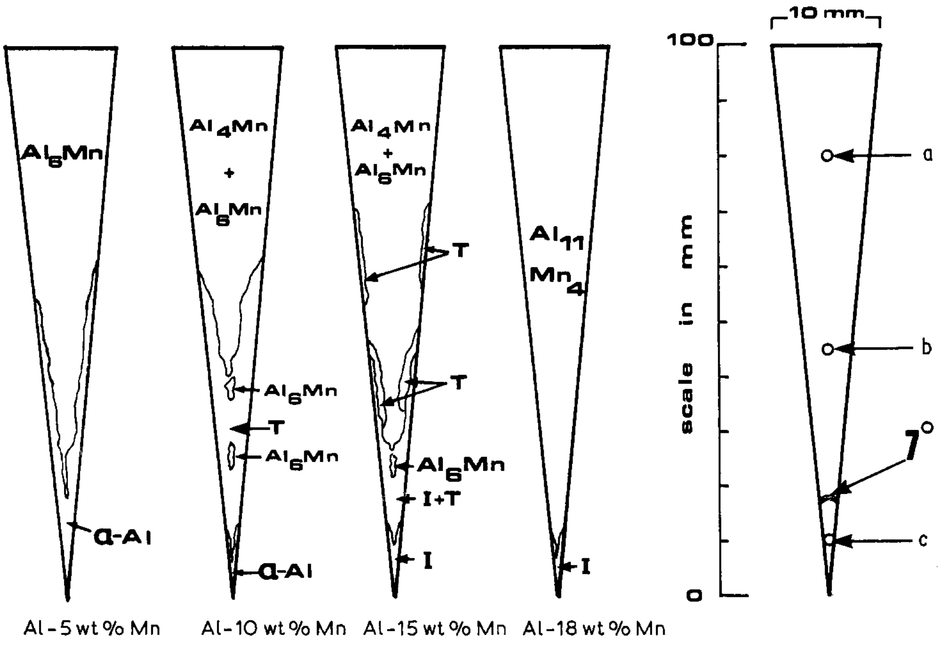

Figure 2 Structure zone location in chill-cast wedges of Al–5 to 18 wt % Mn alloys. α-Al = α-Al solid solution, Al_6Mn = primary or dendritic Al_6Mn, Al_4Mn = primary Al_4Mn, $Al_{11}Mn_4$ = primary LT-$Al_{11}Mn_4$, T = decagonal or T-phase and I = icosahedral phase.

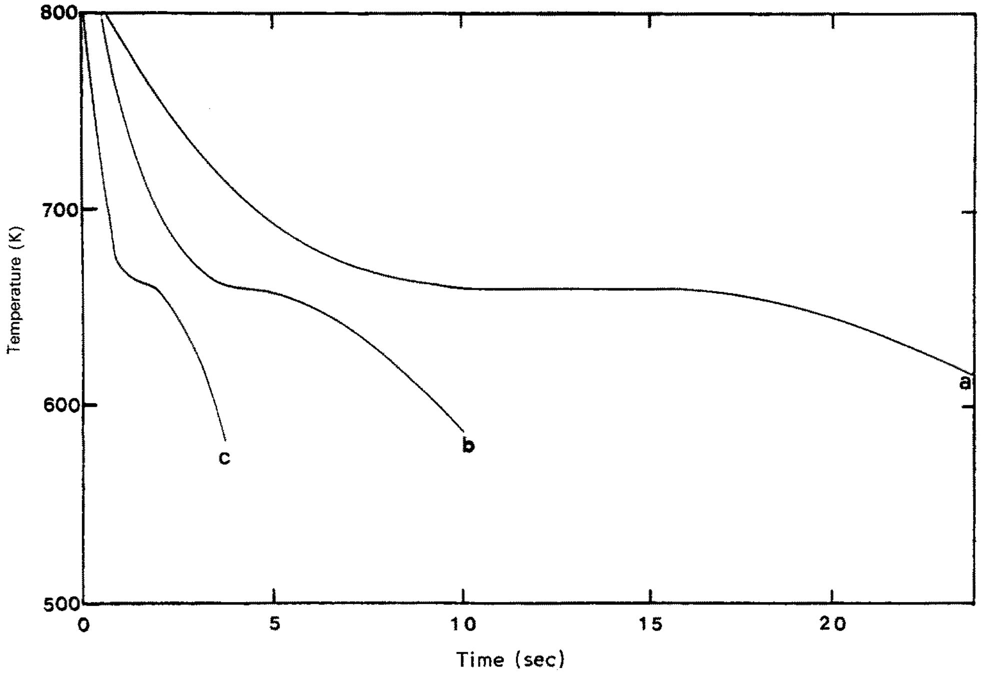

Figure 3 Temperature against time histories for an Al–10 wt % Mn alloy cast into a wedge-shaped copper mould. Thermocouple points (a, b, c) as in Fig. 2.

6. Icosahedral phase, which showed the morphology of isolated equiaxed crystals in an α-Al matrix. They grew radially outward with defined growth directions, as shown in Figs 4g and h, at the narrow end of wedge shaped ingots of Al–15 and 18 wt % Mn. Figure 5e shows the X-ray diffraction pattern of the microstructure containing icosahedral phase, which show also the presence of the decagonal phase. Microanalysis carried out in the icosahedral phase showed a composition of 65.9 wt % Al (79.7 at %) and 34.1 wt % Mn (20.3 at %).

Al_6Mn has been established as a stable equilibrium phase [10]. Al_4Mn was identified as λ-Al_4Mn mainly by its chemical composition and morphology, because

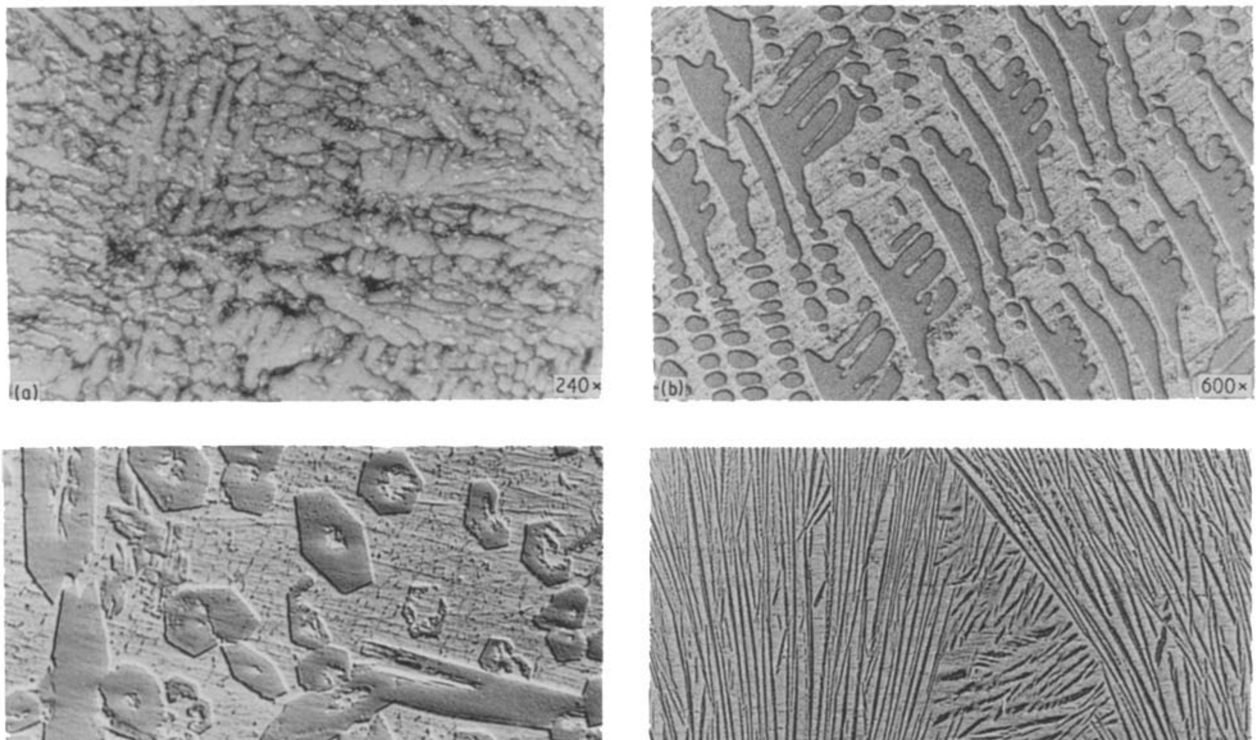

Figure 4 Microstructures observed in chill-cast ingots: (a) Dendritic α-Al solid solution observed in chill-cast wedges of Al–5 wt % Mn; (b) dendritic Al_6Mn in a cellular α-Al solid solution matrix observed in chill cast Al–10 and 15 wt % Mn; (c) primary Al_4Mn in a cellular α-Al solid solution matrix observed in chill-cast wedges of Al–15 wt % Mn; (d) bundles of LT-$Al_{11}Mn_4$ platelets observed in chill-cast wedges of 18 wt % Mn; (e) and (f) decagonal phase together with some dendrites of Al_6Mn (e) and decagonal and icosahedral phase, (f) observed in chill-cast wedges of Al–10 and 15 wt % Mn, respectively; and (g) and (h) icosahedral phase served in chill-cast wedges of Al–15 wt % Mn.

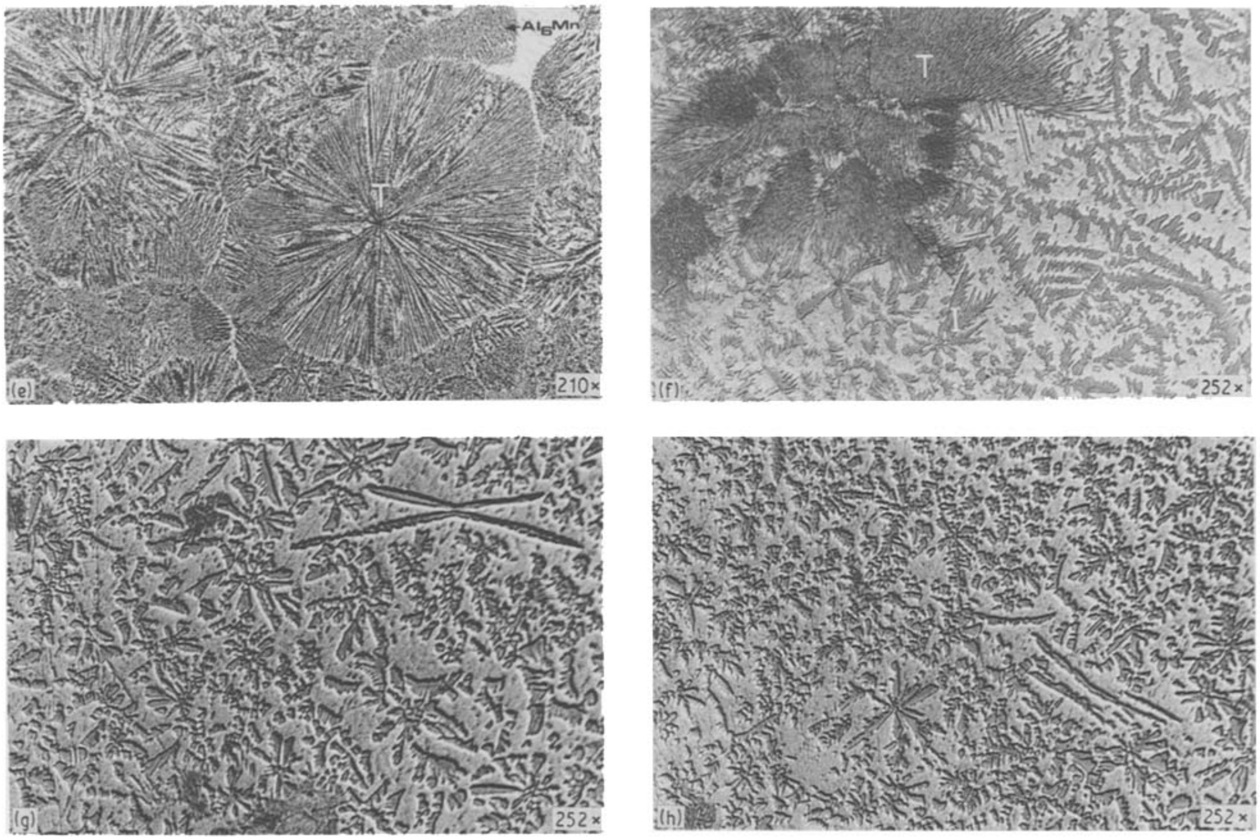

Figure 4 Continued.

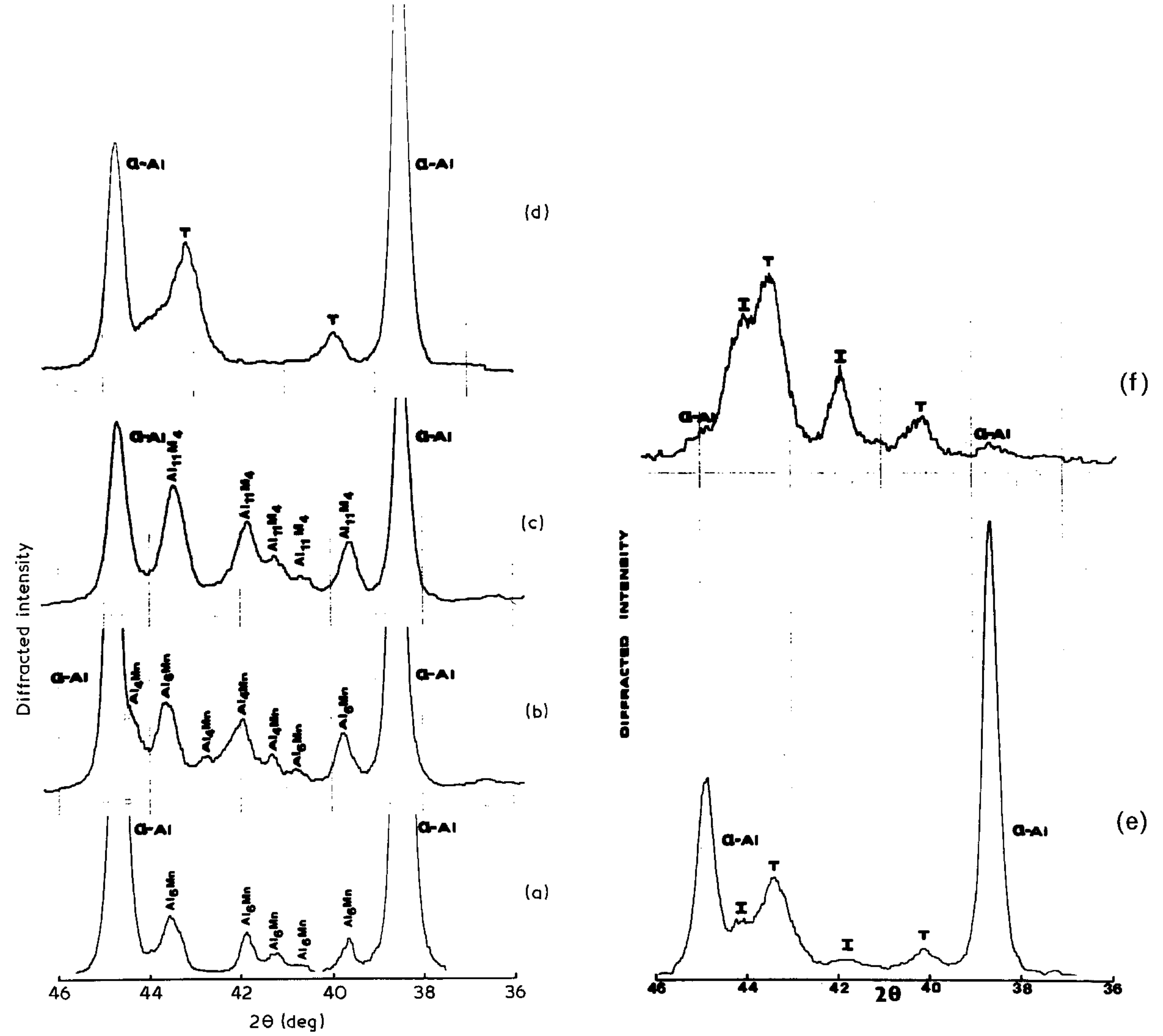

Figure 5 X-ray diffraction patterns of phases observed, for Cu$K\alpha$ radiation in the range $38° < 2\theta < 46°$.

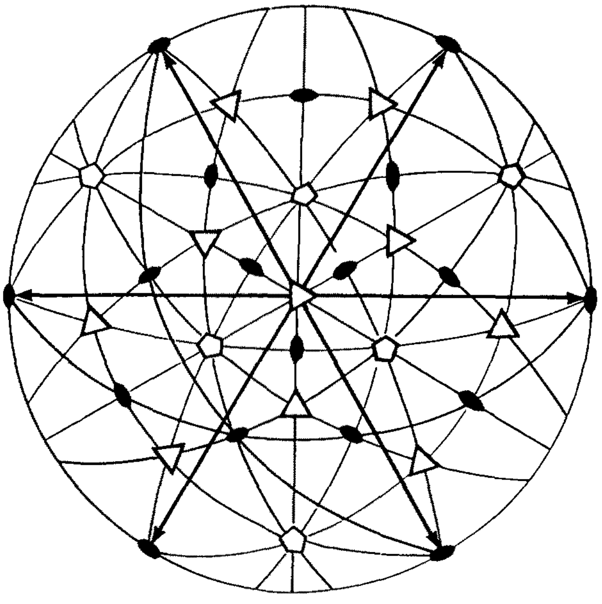

Figure 6 The stereographic projection of the icosahedral group m35 as seen along a three-fold direction.

there are differing reports concerning its crystal structure, i.e. hexagonal with $c = 1.24\,\mathrm{nm}$ and $a = 2.84\,\mathrm{nm}$ [11] or orthorhombic with $a = 0.6795\,\mathrm{nm}$, $b = 0.9343\,\mathrm{nm}$ and $c = 1.3897\,\mathrm{nm}$ [12]. LT-$Al_{11}Mn_4$ [13], once again was identified by its chemical composition but also by X-ray diffractometry and morphology. These intermetallics were observed to have formed at cooling rates as low as $\sim 20\,\mathrm{K\,sec^{-1}}$ during solidification and are stable alloy phases of the Al–Mn system.

The other two intermetallic phases, the decagonal and icosahedral are metastable (as was shown for Al–28 and 32 wt % Mn splat-cooled alloys, by TEM *in situ* heating at 300° C, for 8 h [14]), which were accompanied (as for the other three intermetallics) predominantly by α-Al. This contrasts with the X-ray diffractogram shown in Fig. 5f for an Al–32 wt % Mn splat, in which the predominant phases are the decagonal and icosahedral, with nearly total suppression of α-Al (gun technique, $\dot{T} - 10^7\,\mathrm{K\,sec^{-1}}$) where $\dot{T}$ = cooling rate). The predominant metastable phase was the decagonal, formed at cooling rates of $\sim 47\,\mathrm{K\,sec^{-1}}$ in ingots of Al–10 and 15 wt % Mn. Recently, the decagonal phase was reported [6] to be formed at cooling rates of $25\,\mathrm{K\,sec^{-1}}$ in Al–15 wt % Mn emulsified droplets ($\sim 75\,\mu\mathrm{m}$ in diameter). However, the main intermetallic phase in those samples was Al_4Mn, as was indicated by their X-ray diffractogram. These observations taken together suggest that the formation of Al_4Mn at $25\,\mathrm{K\,sec^{-1}}$ is suppressed in favour of the decagonal phase when the cooling rate is increased to $50\,\mathrm{K\,sec^{-1}}$.

The icosahedral phase was detected in regions where the cooling rate was $\sim 150\,\mathrm{K\,sec^{-1}}$ (in comparison with $500\,\mathrm{K\,sec^{-1}}$ reported in [6]), showing dendritic morphology similar to that reported [5] for electron beam melting experiments. Continuous dendrite arms are seen for the icosahedral phase when the plane of view lies perpendicular to the three-fold (Fig. 4h) symmetry axis. Comparison of the angles between dendrites with a stereographic projection of the icosahedral phase suggest that they grow from a central nucleus along the two-fold (Fig. 6) symmetry axes.

4. Conclusions

1. At a cooling rate of $\sim 21\,\mathrm{K\,sec^{-1}}$ during solidification, Al_6Mn is the initial phase to form in Al–5 wt % Mn, while Al_4Mn is the initial phase to form in Al–10 and 15 wt % Mn.

2. The decagonal phase formed at a cooling rate of $\sim 50\,\mathrm{K\,sec^{-1}}$ in ingots containing 10 and 15 wt % Mn, while in regions of these ingots where the cooling rate was $\sim 150\,\mathrm{K\,sec^{-1}}$, the icosahedral phase was formed. This cooling rate is the lowest value reported to result in formation of the icosahedral phase in the Al–Mn system.

3. The icosahedral phase formed in the alloy containing 15 wt % Mn in competition with the decagonal phase, which was eventually replaced by the icosahedral phase at sufficiently high cooling rate ($\sim 150\,\mathrm{K\,sec^{-1}}$).

References

1. D. SHECHTMAN, I. BLECH, D. GRATIAS and J. W. CAHN, *Phys. Rev. Lett.* **53** (1984) 1951.
2. D. SHECHTMAN, R. J. SHAEFER and F. S. BIANCANIELLO, *Met. Trans. A* **15A** (1984) 1987.
3. K. CHATTOPADHYAY, S. RANGANATHAN, G. N. SUBBUNNA and N. THANGARAJ, *Scripta Met.* **19** (1985) 767.
4. D. SHECHTMAN and I. A. BLECH, *Met. Trans. A* **16A** (1985) 1005.
5. R. J. SCHAEFER, L. A. BENDERSKY, D. SHECHTMAN, W. J. BOETTINGER and F. S. BIANCANIELLO, *ibid.* **17A** (1986) 2117.
6. B. A. MUELLER, R. J. SCHAEFER and J. H. PEREPEZKO, *J. Mater. Res.* **2** (1987) 809.
7. H. JONES, *Aluminium* **54** (1978) 274.
8. J. CAMPBELL, P. S. NYHOLM and B. R. KNOTT, *A.F.S. International Cast Metals Research J.* **12** (1976) 9–12.
9. L. F. MONDOLFO, in "Aluminium Alloys, Structure and Properties" (Butterworths, London, 1976) p. 324.
10. G. V. RAYNOR and W. HUME-ROTHERY, *J. Inst. Met.* **69** (1943) 415.
11. W. HOFMANN, *Aluminium* **20** (1938) 865.
12. T. ONISHI and Y. NAKETANI, *J. Jpn Inst. Light Metals* **25** (1975) 253.
13. N. Kh. ABRIKOSOV, L. IVANOVA and V. A. DANIL'CHENKO, *Inorg. Mater.* 7(6) (1971) 933.
14. J. A. JUAREZ-ISLAS, PhD thesis, Department of Metallurgy, University of Sheffield, 1986.
15. J. W. CAHN, D. SHECHTMAN and D. GRATIAS, *J. Mater. Res.* **1**(1) (1986) 13.

Received 29 March
and accepted 29 July 1988